

## SUPPORTING INFORMATION

### Selective adsorption behavior of carbon dioxide in OH- functionalized metal-organic framework materials\*\*

Jinjie Qian,<sup>\*ab</sup> Jinni Shen,<sup>b</sup> Qipeng Li,<sup>b</sup> Yue Hu<sup>\*a</sup> and Shaoming Huang<sup>\*a</sup>

<sup>a</sup>College of Chemistry and Materials Engineering, Wenzhou University, Wenzhou 325035, P. R. China.

<sup>b</sup>State Key Laboratory of Structure Chemistry, Fujian Institute of Research on the Structure of Matter,  
Chinese Academy of Sciences, Fuzhou, Fujian 350002, China.

*\*To whom correspondence should be addressed: E-mail: [jinjieqian@wzu.edu.cn](mailto:jinjieqian@wzu.edu.cn); [yuehu@wzu.edu.cn](mailto:yuehu@wzu.edu.cn);  
[smhuang@wzu.edu.cn](mailto:smhuang@wzu.edu.cn); Tel: 86-577-88373064.*

#### Table of Content

|   |         |
|---|---------|
| S1. Materials and Methods                               | S1-S3   |
| S2. SEM Images  | S4      |
| S3. TGA data  | S5-S6   |
| S4. PXRD Patterns                                       | S7-S8   |
| S5. N <sub>2</sub> Isotherms and Pore Size Distribution | S9-S15  |
| S6. The Heat of Adsorption                              | S18-S27 |
| S7. Energy Band Dispersion                              | S28     |

## S1. Materials and Methods

**1.1. Materials and Instruments.** Reactions were carried out in 35 ml vials/autoclaves under autogenous pressure. All the reactants are of reagent-grade quality and used as commercially purchased without further purification. The power X-ray diffraction patterns (PXRD) were collected by a Bruker D8 Advance using Cu K $\alpha$  radiation ( $\lambda = 0.154$  nm). Single gas adsorption measurements were performed in the Accelerated Surface Area and Porosimetry 2020 (ASAP2020, where the bulk **InOF-1** and **AlOF-1** materials were determined in a clean ultra high vacuum system and the N<sub>2</sub> sorption measurement was performed at 77 K and the CO<sub>2</sub> sorption test was conducted at 273 K, 283 K and 295 K. Thermogravimetric analyses were recorded on a NETZSCH STA 449C unit at a heating rate of 10 °C·min<sup>-1</sup> under flowing nitrogen atmosphere. Scanning transmission electron microscopy (STEM) and energy dispersive X-ray spectroscopy (EDS) analyses were carried out under JEOL JEM-2100F microscope operating at an accelerating voltage of 200 kV.

**1.2. Synthesis of [In<sub>2</sub>(OH)<sub>2</sub>(BPTC)] (InOF-1).** A mixture of In(NO<sub>3</sub>)<sub>3</sub>·5H<sub>2</sub>O (0.40 mmol, 120 mg) and H<sub>4</sub>BPTC (0.10 mmol, 33 mg) in N,N'-dimethylformamide (DMF) (5 ml) and CH<sub>3</sub>CN (5 ml) with an additional 0.2 ml HNO<sub>3</sub> (65 wt %) was placed in a 25 ml vial, which was heated at 85 °C for 3 days, and cooled to room-temperature. After washed by fresh DMF, the colorless crystals **InOF-1** were obtained in *ca.* 45% yield based on In(NO<sub>3</sub>)<sub>3</sub>·5H<sub>2</sub>O. Elemental analysis was calculated for **InOF-1**: C, 32.58%; H, 1.37%. Found: C, 32.51%; H, 1.51%. The phase purity of the sample was confirmed by powder X-ray diffraction (Figure S6).

**1.3. Synthesis of [Al<sub>2</sub>(OH)<sub>2</sub>(BPTC)] (AlOF-1).** Silimar to the synthesis procedure of **InOF-1**, the mixture of Al(NO<sub>3</sub>)<sub>3</sub>·9H<sub>2</sub>O (0.10 mmol, 38 mg) and H<sub>4</sub>BPTC (0.10 mmol, 33 mg) in deionized H<sub>2</sub>O (5 ml) with an additional 0.1 ml HNO<sub>3</sub> (65 wt %), but was sealed in a 30 ml autoclave, which was heated at 200 °C for 2 hours, and cooled

to room-temperature. After washed by fresh DMF, the amorphous powder of **AIOF-1** was obtained in *ca.* 50% yield based on the salt. The phase purity of the sample was also confirmed by powder X-ray diffraction (Figure S6).

**1.4. Synthesis of [Ga<sub>2</sub>(OH)<sub>2</sub>(BPTC)] (GaOF-1).** According to the previous literature [Inorg. Chem., 2016, 55, 1076–1088], the mixture of Ga(NO<sub>3</sub>)<sub>3</sub>·(0.15 mmol, 38 mg) and H<sub>4</sub>BPTC (0.07 mmol, 23.1 mg) in a 2:5:1 mixture of DMF, THF, and water (8 mL) with an additional 0.1 ml HCl, but was sealed in a 35 ml vial, which was holded at 85 °C for 3 days, and cooled to room-temperature. After washed by fresh DMF and EtOH, and dried in air. Finally, the crystalline micropowder of **GaOF-1** was collected in *ca.* 68% yield based on the gallium salt. The phase purity of the sample was also confirmed by powder X-ray diffraction (Figure S6).

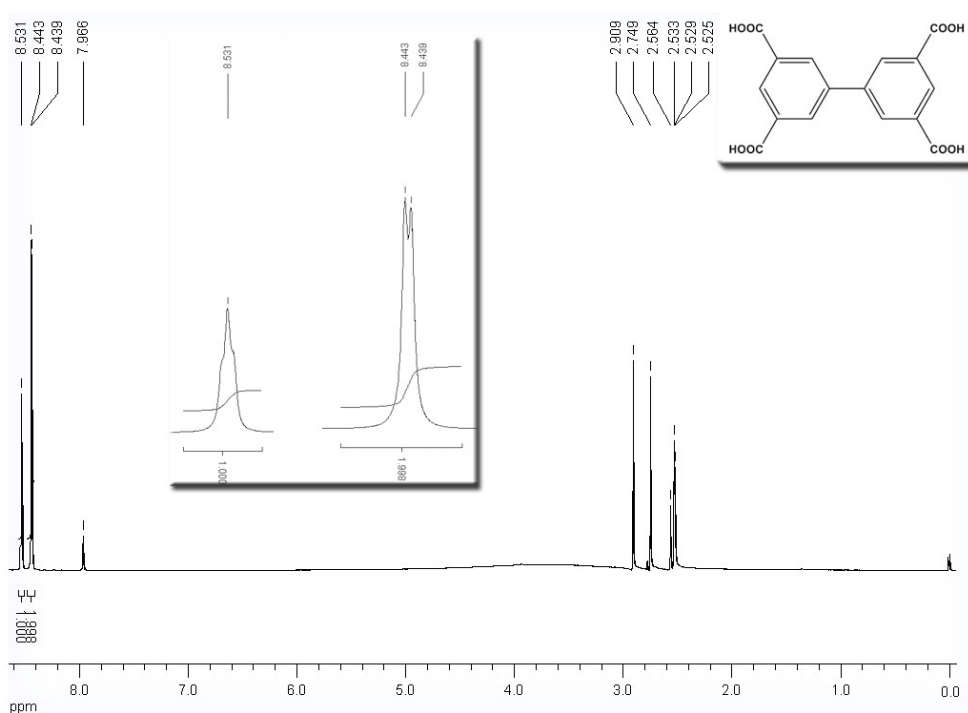


**Figure S1.** <sup>1</sup>H-NMR spectrum of the H<sub>4</sub>BPTC ligand was measured in DMSO-d<sub>6</sub>.

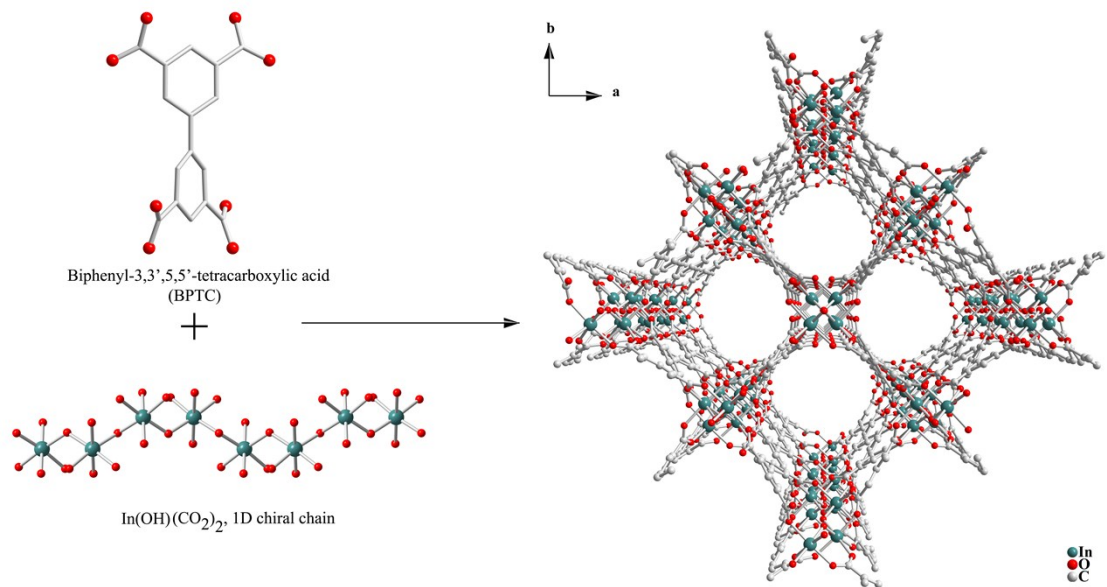


**Figure S2.** The formation of  $[\text{In}_2(\text{OH})_2(\text{BPTC})]$ -based hydroxyl-functionalized tetragonal channels for **InOF-1** structure as well as its Al-/Ga-based isostructures in the  $c$  axis.

## S2. SEM Images

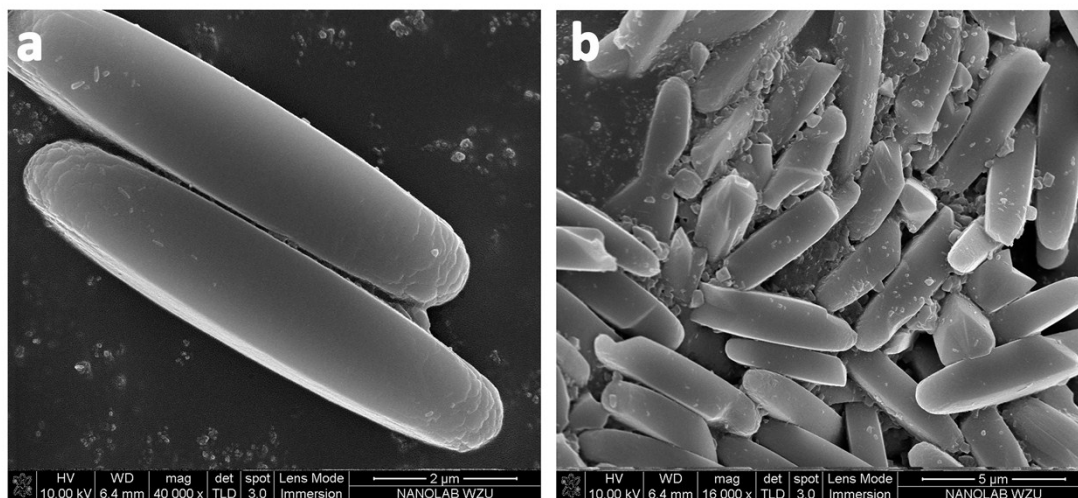


**Figure S3.** SEM images shows the rice-like particles for **InOF-1**.

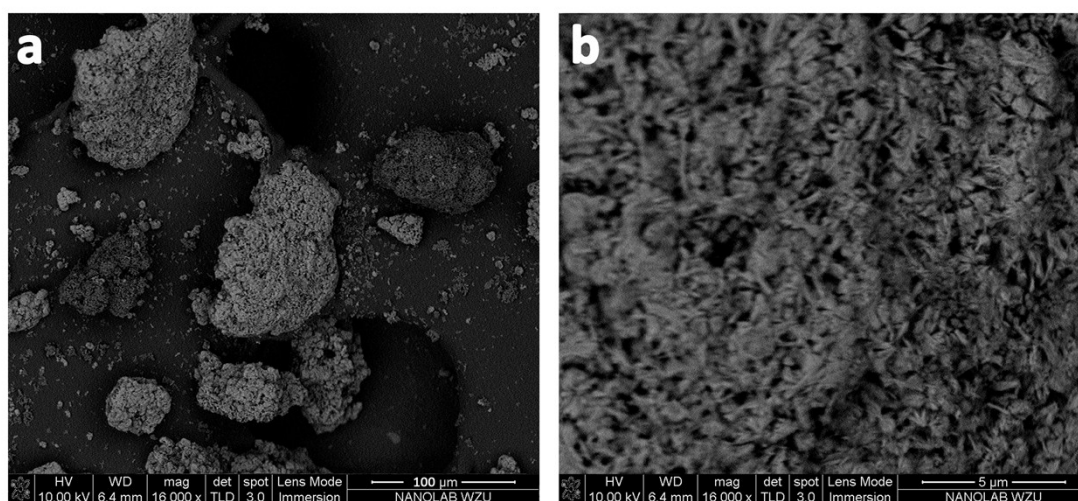


**Figure S4.** SEM images shows the irregular morphology for amorphous **AlOF-1**.

### S3. TGA data

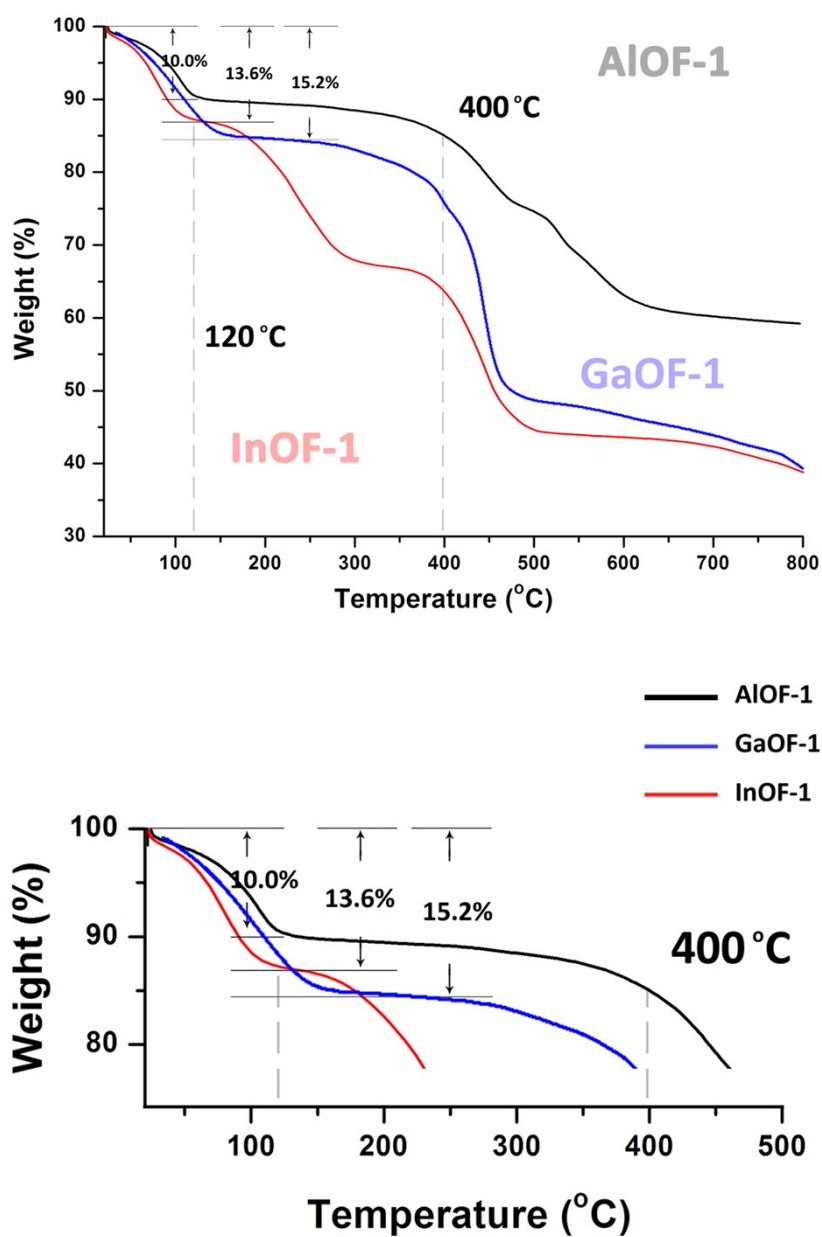


**Figure S5.** TGA curves for AIOF-1, GaOF-1 and InOF-1 samples. In this context, we use the temperature of 120 °C to activate the microcrystals to obtain desolvated materials for the following physisorption test. The bottom is the magnified TGA zone between 25 and 800 °C.

The thermogravimetric analysis (TGA) was carried out on polycrystalline samples of **AlOF-1**, **GaOF-1** and **InOF-1** in the temperature range from 25 to 800 °C in the flowing N<sub>2</sub> atmosphere with a heating rate of 5 °C min<sup>-1</sup> (please see above).

At the beginning, the TGA curves display a weight loss of ~10.0%/13.6%/15.2% before reaching a structural equilibrium (we take 120 °C as the degas temperature prior to gas sorption), which can be reasonably attributed to the loss of guest uncoordinated water and EtOH molecules (EtOH solvent is used to exchange the isolated and disordered H<sub>2</sub>O and DMF prior to the desolvation) in the pores. After that, to our surprise, **InOF-1** continues to lose the incompletely removed DMF molecules in the temperature range of 150~300 °C, while Al-/Ga-based isostructures remain a plateau until 400 °C.

Finally, with the increasing temperature (>400 °C), the main frameworks of these 3 materials are starting to collapse, and the coordination bonds between Al(III)/Ga(III)/In(III) centres and BPTC<sup>4-</sup> ligands are going to break down gradually, the BPTC ligands and coordinated OH groups are going to seriously deteriorate, which is presented in TGA curves with a continuous weight loss until 800 °C.

We notice that our as-prepared **GaOF-1** sample continues to lose weight of 15.2% at 250 °C, while our degas temperature is 120 °C. Thus the TGA plot well explains the incomplete activation which leads to the moderate gas adsorption behaviour of the Ga-based material due to the inability to vacate the guest solvent from the 1-dimensional channels. Meanwhile, we think it is acceptable to take the same degas temperature of 120 °C to desolvate all 3 materials, then do the comparative gas sorption capacity.

## S4. PXRD Patterns

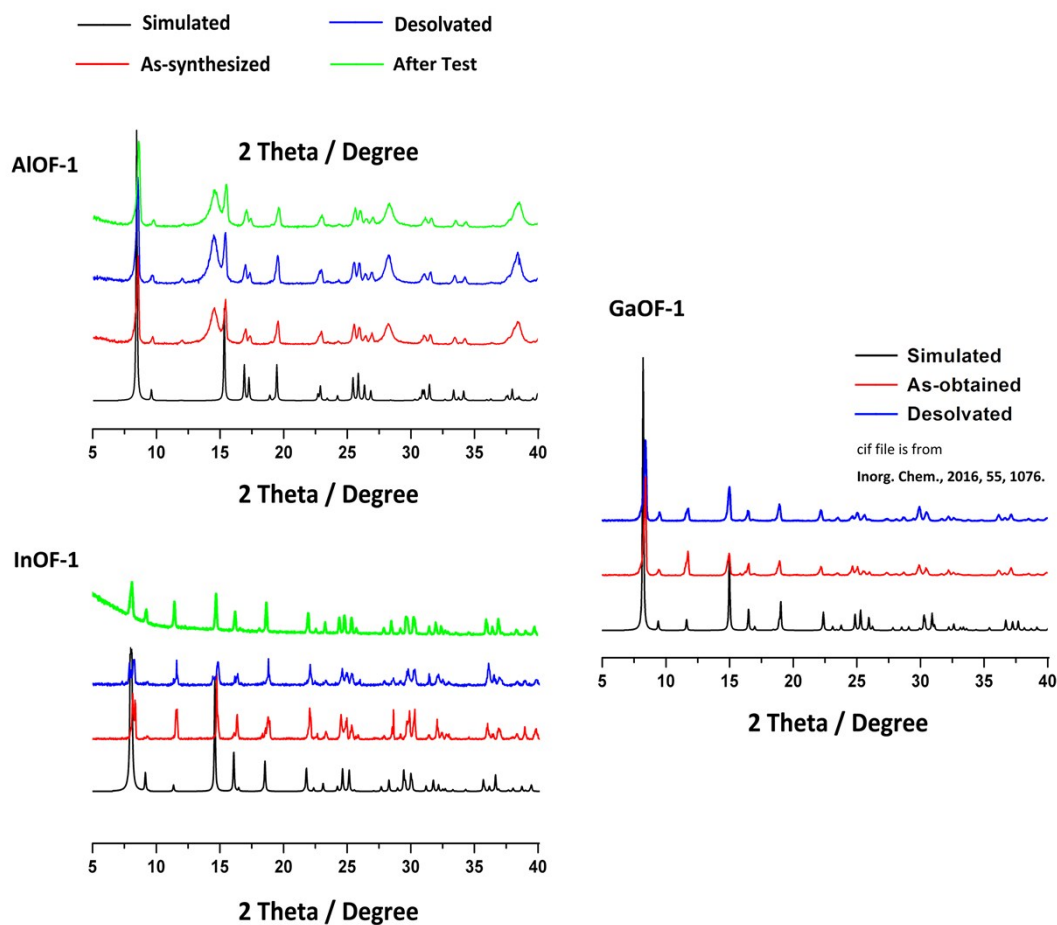


**Figure S6.** PXRD patterns of **AlOF-1**, **GaOF-1** and **InOF-1**: simulated from the crystallographic information file (black); from the as-prepared sample (red); from the desolvated sample activated at 120 °C (blue); from the samples after the sorption test (green).

Refer to the synthesis section in SI on Page S1-S2 above, we have obtained the **AlOF-1** microcrystals in a totally green procedure where the mixture of  $\text{Al}(\text{NO}_3)_3 \cdot 9\text{H}_2\text{O}$  and  $\text{H}_4\text{BPTC}$  in deionized  $\text{H}_2\text{O}$  (5 ml) sealed in an autoclave and heated at 200 °C for 2 hours.

In our cases, we learn that the PXRD patterns of as-obtained samples always exhibit additional broad peaks at 14.48 and 28.28° (plz see below), while the other diffraction peaks are well fitted to the simulated one.

Therefore, we believe we have successfully prepared the target compound. On the other hand, we assume that the additional peaks around  $\sim 14$  and  $\sim 28^\circ$  might be derived from the amorphous carbon and/or side-product polymer with poor crystallinity in the very high temperature  $200^\circ\text{C}$  in our synthesis procedure.

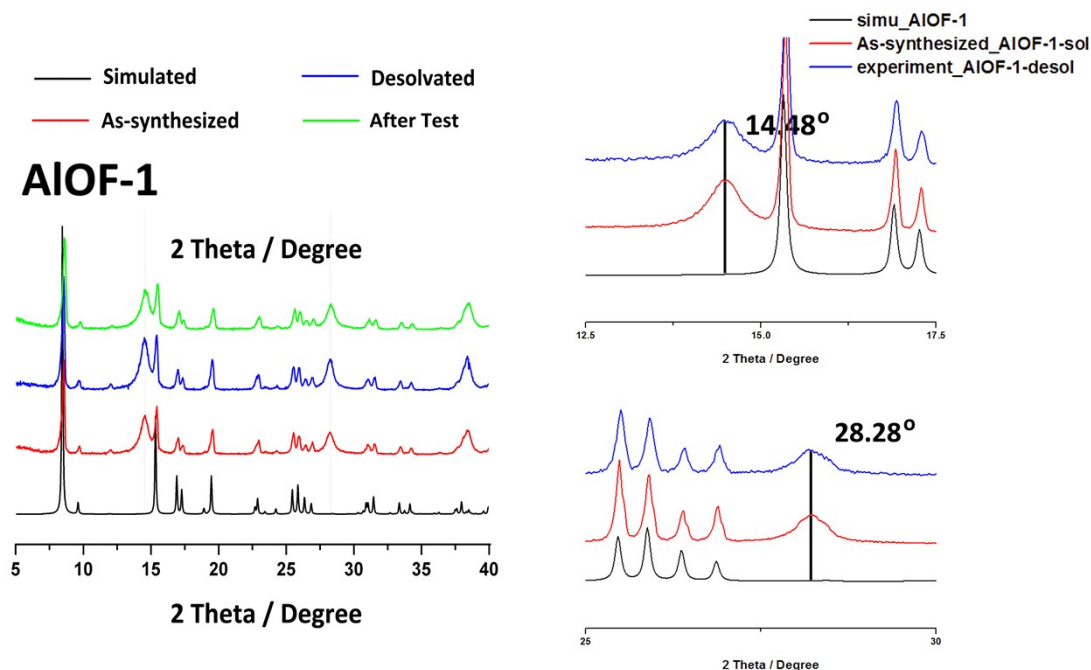


**Figure S7 (in Supporting Information).** PXRD pattern of AIOF-1 with the magnified zone in  $12.5\text{--}17.5^\circ$ ,  $25\text{--}30^\circ$ : simulated from the crystallographic information file (black); from the as-prepared sample (red); from the desolvated sample (blue); from the samples after the sorption test (green).

## S5. Gas Isotherms and Pore Size Distribution

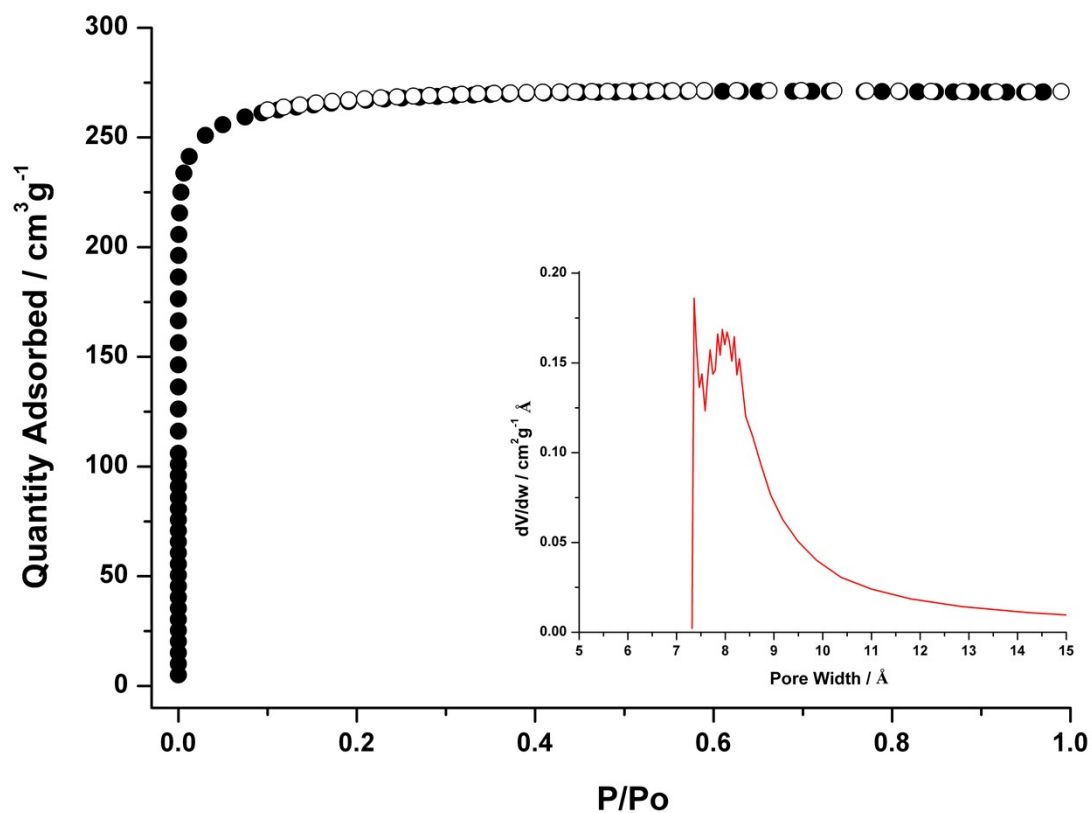


**Figure S8.** (a) Experimental  $N_2$  sorption isotherms at 77 K for the bulk **InOF-1** samples; ● adsorption, ○ desorption. Inset shows the pore size distribution incremental pore volume (V) vs. pore width (d)

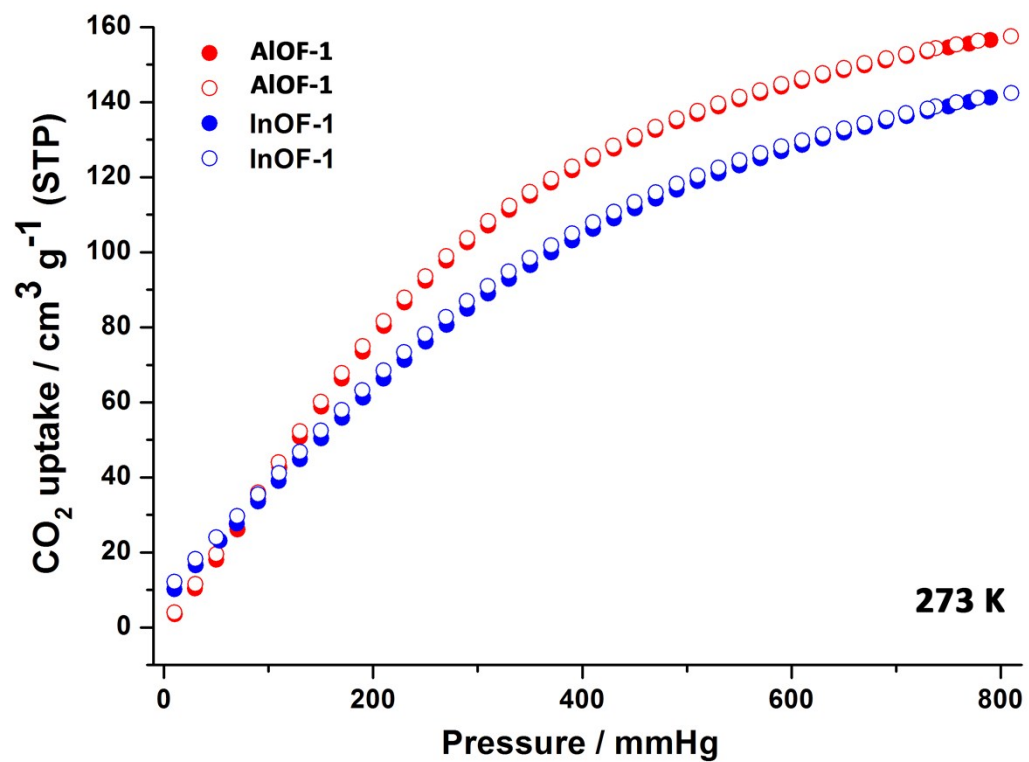


Figure S9. CO<sub>2</sub> isotherms at 273 K for InOF-1 and AIOF-1.

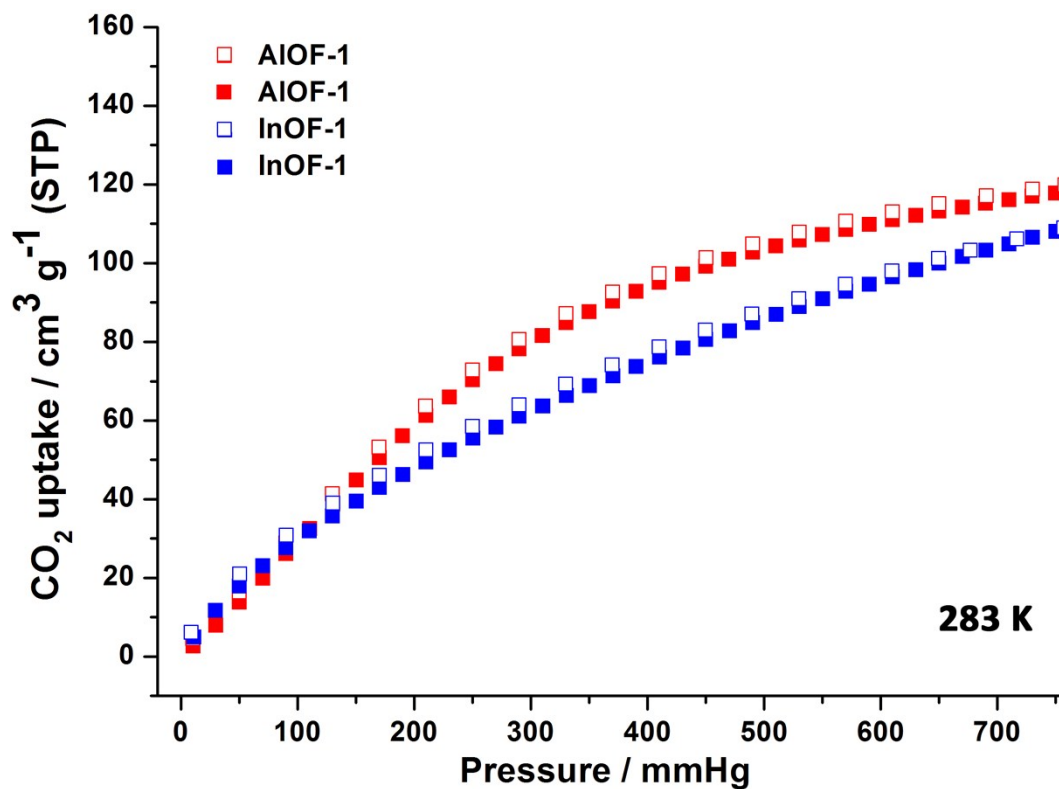


Figure S10. CO<sub>2</sub> isotherms at 283 K for InOF-1 and AIOF-1.

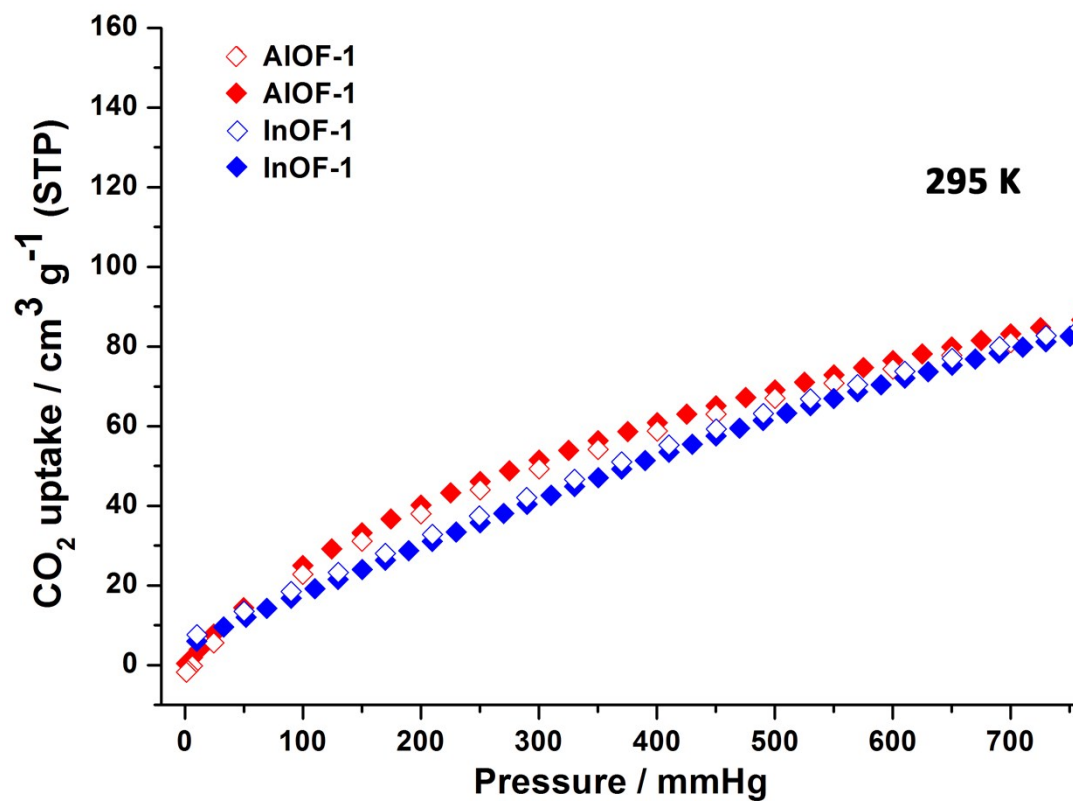


Figure S11. CO<sub>2</sub> isotherms at 295 K for InOF-1 and AIOF-1.

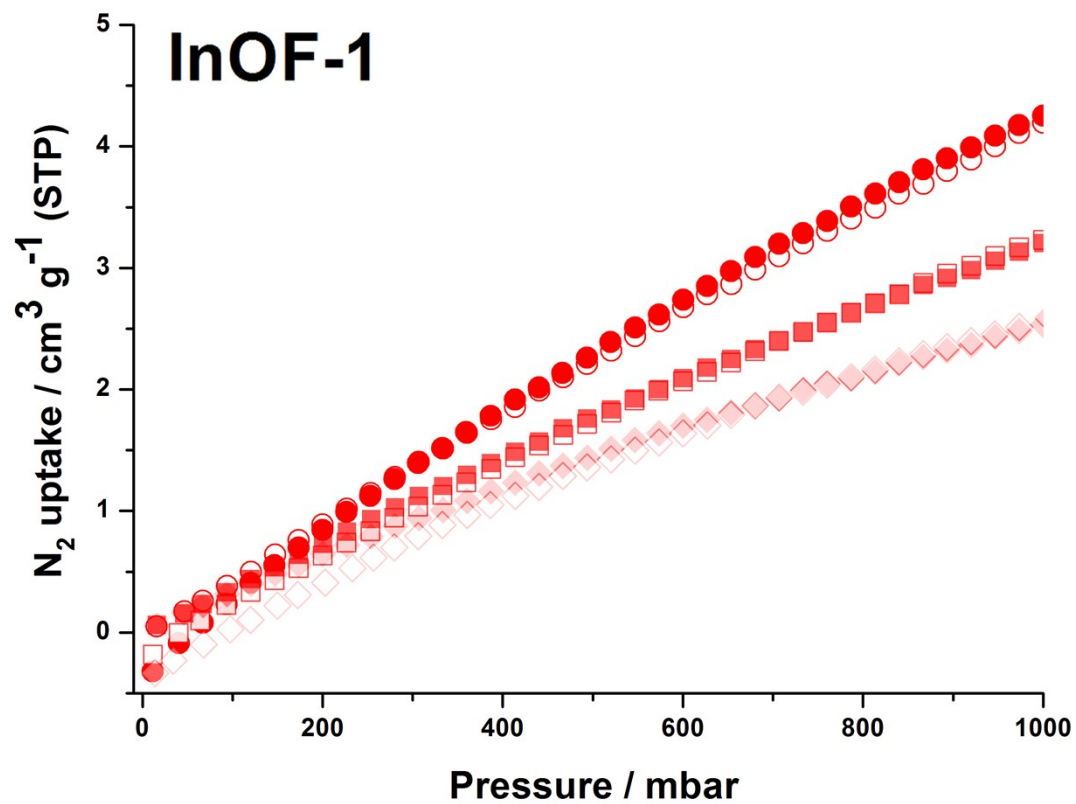


Figure S12. N<sub>2</sub> isotherms at 273-295 K for the activated InOF-1.

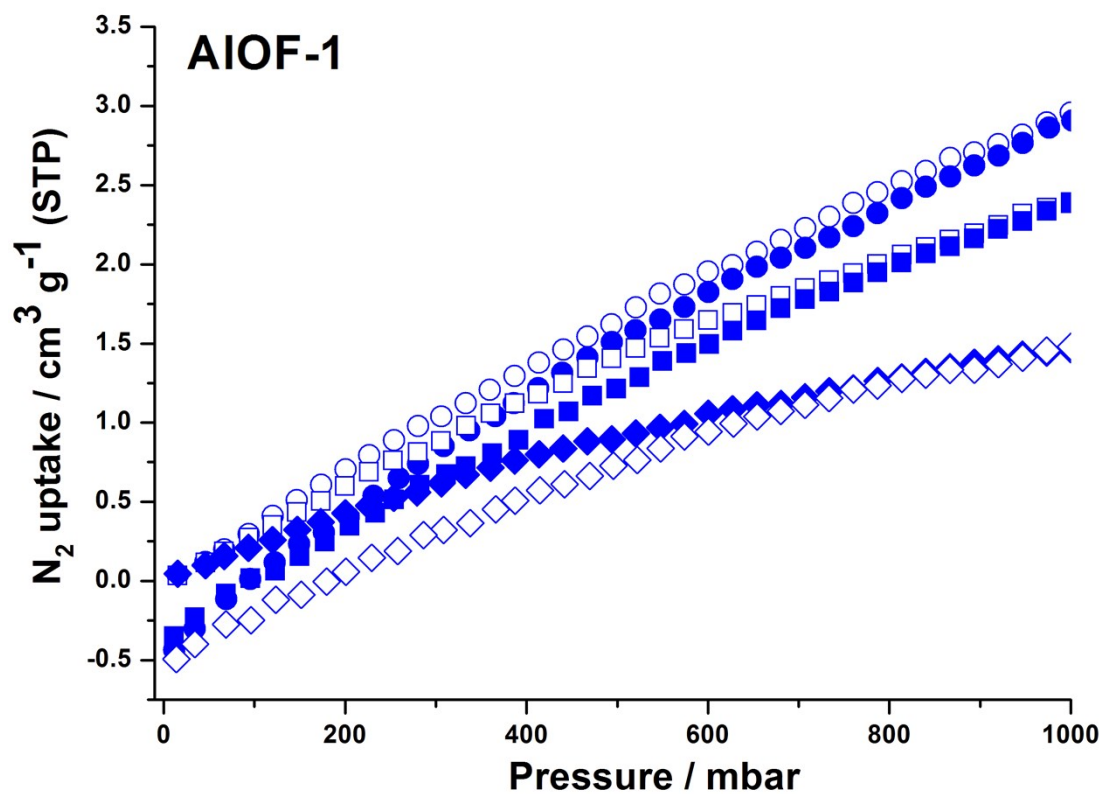
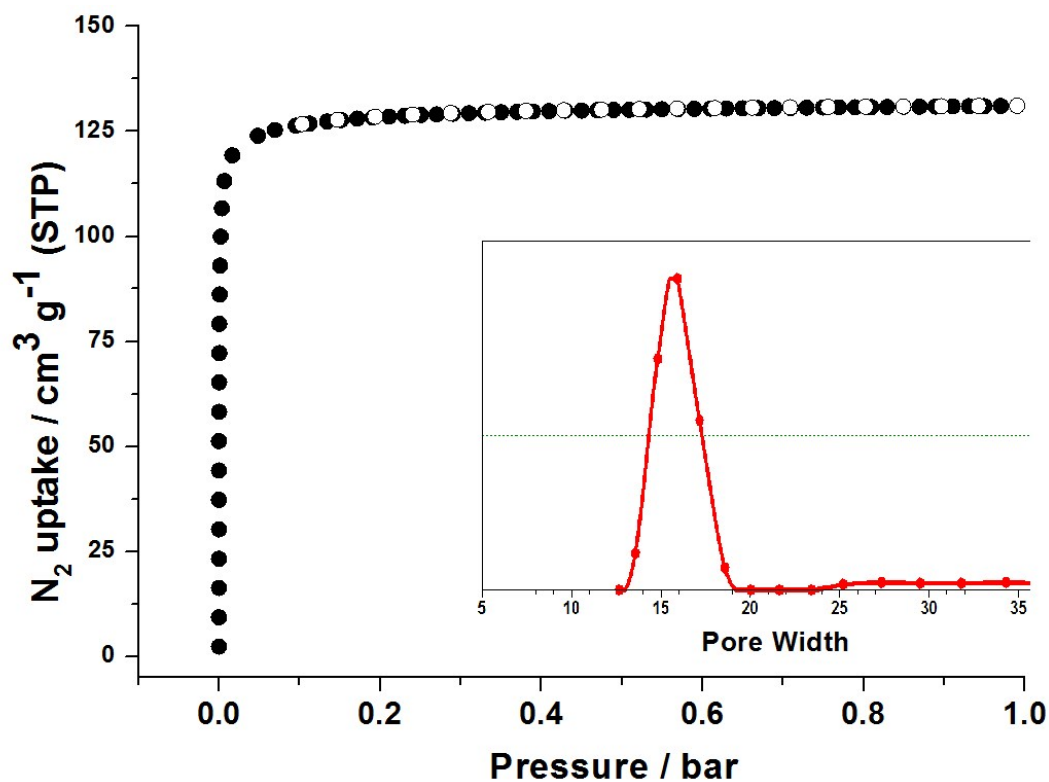
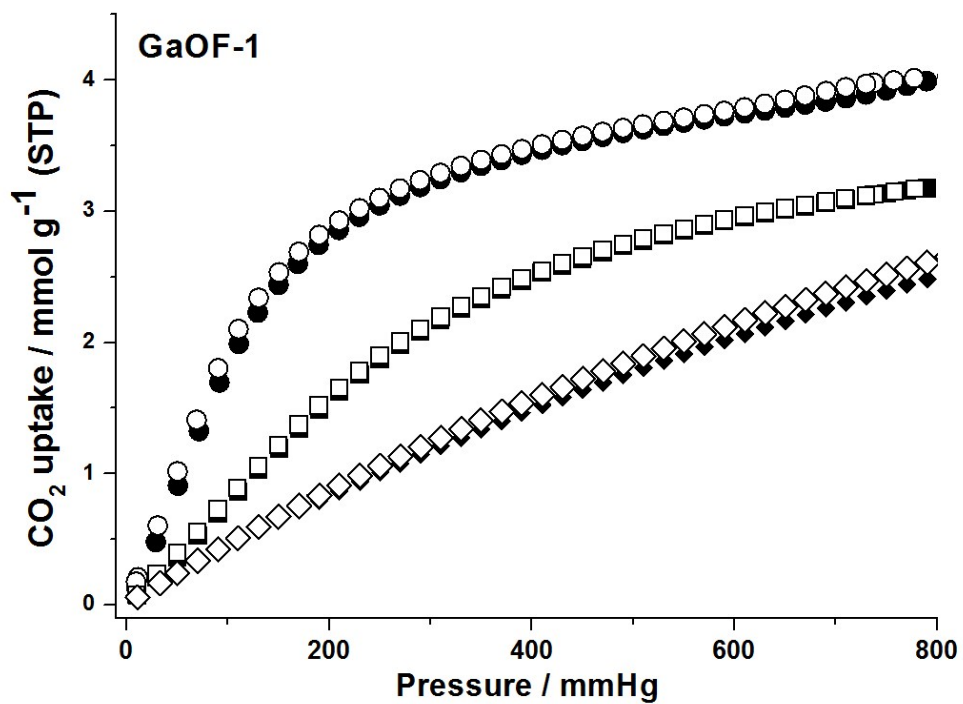


Figure S13.  $N_2$  isotherms at 273-295 K for the activated AIOF-1.



**Figure S14.** (a) Experimental N<sub>2</sub> sorption isotherms at 77 K for the as-prepared GaOF-1 samples; ● adsorption, ○ desorption. Inset shows the pore size distribution incremental pore volume (V) vs. pore width (d))



**Figure S15.** CO<sub>2</sub> adsorption/desorption isotherms at 273-295 K for the activated GaOF-1.

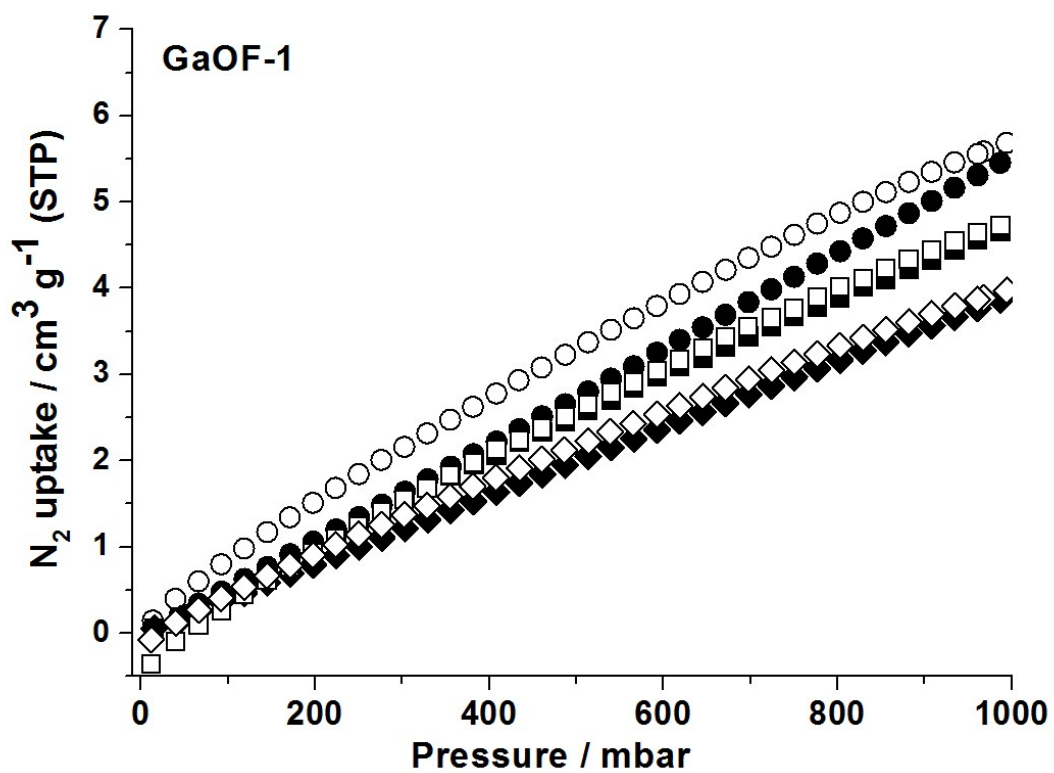


Figure S16. N<sub>2</sub> isotherms at 273-295 K for the desolvated GaOF-1.

## S6. The Heat of Adsorption for CO<sub>2</sub>

### Heat of Adsorption (kJ mol<sup>-1</sup>)

CO<sub>2</sub> isotherms (adsorption and desorption) measured at 283 and 295 K for **AlOF-1**, **GaOF-1** and **InOF-1** were fitted to the following Equation 1.

The adsorption isotherm is represented by

$$\ln (P/P_0) = q_i/RT + C \quad (1)$$

where

$q_i$  = isosteric heat of adsorption

$C$  = unknown constant

The isosteric heat of adsorption,  $q_i$  is determined by finding the slope of  $\ln (P/P_0)$  as a function of  $1/RT$  for a set of isotherms measured at different temperatures.

$$y = \ln(x) + 1/k * (a_0 + a_1 * x + a_2 * x^2 + a_3 * x^3 + a_4 * x^4 + a_5 * x^5) + (b_0 + b_1 * x + b_2 * x^2)$$

| <b>AIOF-1</b> |            | <b>Value</b>       | <b>Standard Error</b> |
|---------------|------------|--------------------|-----------------------|
| <b>ln(P)</b>  | <b>a0*</b> | <b>-1882.76547</b> | <b>117.29814</b>      |
|               | <b>a1*</b> | <b>68.22595</b>    | <b>2.82086</b>        |
|               | <b>a2*</b> | <b>-0.08619</b>    | <b>0.01838</b>        |
|               | <b>a3*</b> | <b>-6.49126E-4</b> | <b>1.04348E-4</b>     |
|               | <b>a4*</b> | <b>2.61955E-6</b>  | <b>4.92381E-7</b>     |
|               | <b>a5*</b> | <b>-3.71909E-9</b> | <b>8.31675E-10</b>    |
|               | <b>b0*</b> | <b>7.18711</b>     | <b>0.41244</b>        |
|               | <b>b1*</b> | <b>-0.24493</b>    | <b>0.00989</b>        |
|               | <b>b2*</b> | <b>5.47894E-4</b>  | <b>5.20782E-5</b>     |
|               | <b>k</b>   | <b>283</b>         | <b>0</b>              |
|               | <b>k</b>   | <b>295</b>         | <b>0</b>              |

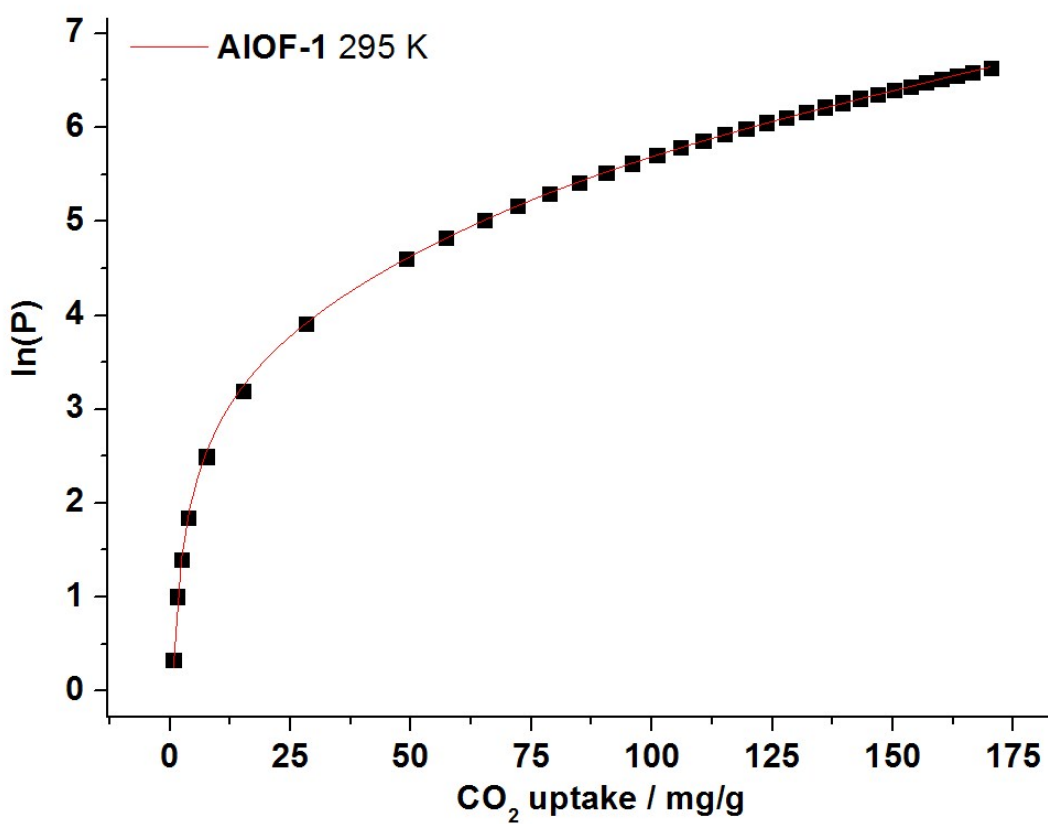
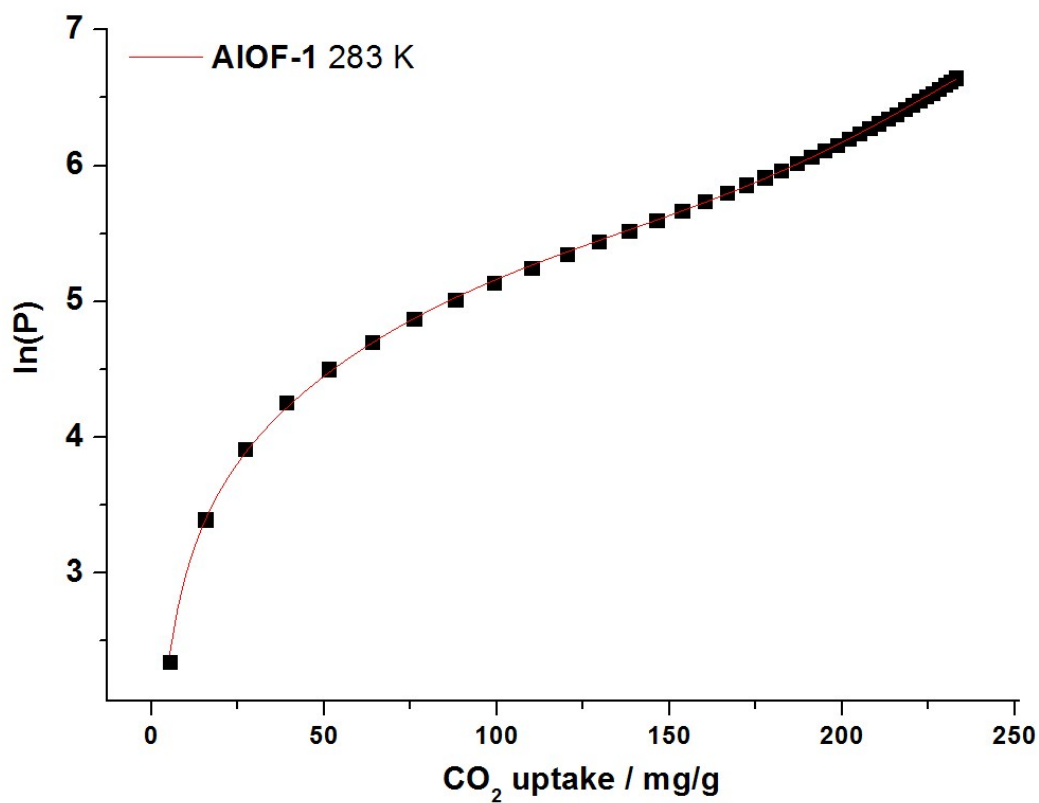
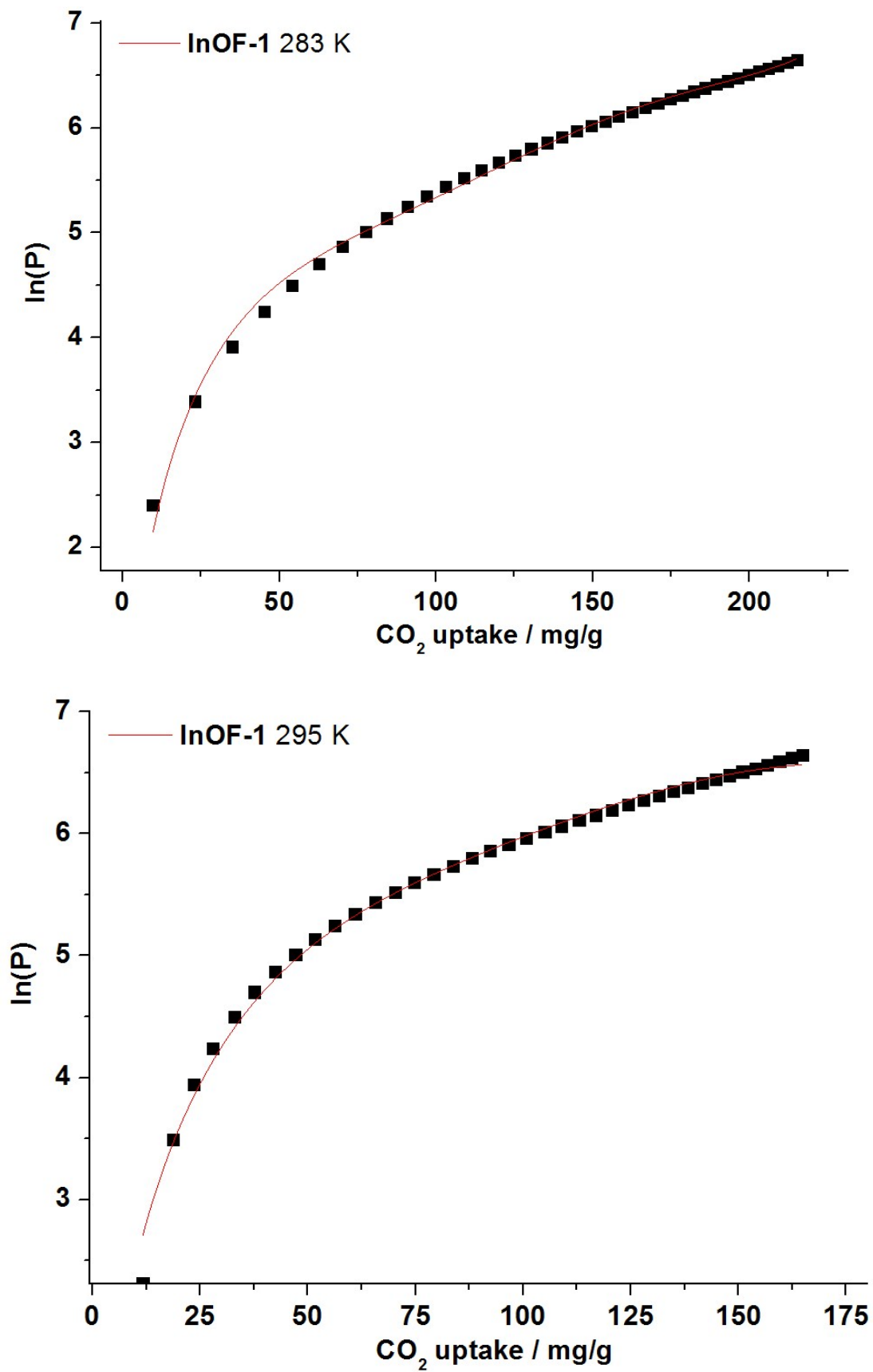


Figure S17. Nonlinear curve fitting of CO<sub>2</sub> adsorption isotherms for AIOF-1 at 283 K and 295 K.

| <b>InOF-1</b> |            | <b>Value</b>       | <b>Standard Error</b> |
|---------------|------------|--------------------|-----------------------|
| <b>ln(P)</b>  | <b>a0*</b> | <b>-1440.68115</b> | <b>561.08062</b>      |
|               | <b>a1*</b> | <b>-53.39589</b>   | <b>12.84085</b>       |
|               | <b>a2*</b> | <b>0.0295</b>      | <b>0.07764</b>        |
|               | <b>a3*</b> | <b>0.00315</b>     | <b>6.6759E-4</b>      |
|               | <b>a4*</b> | <b>-1.30938E-5</b> | <b>3.23055E-6</b>     |
|               | <b>a5*</b> | <b>2.02784E-8</b>  | <b>5.70782E-9</b>     |
|               | <b>b0*</b> | <b>4.45635</b>     | <b>1.95467</b>        |
|               | <b>b1*</b> | <b>0.25186</b>     | <b>0.0457</b>         |
|               | <b>b2*</b> | <b>-0.00132</b>    | <b>2.35841E-4</b>     |
|               | <b>k</b>   | <b>283</b>         | <b>0</b>              |
|               | <b>k</b>   | <b>295</b>         | <b>0</b>              |



**Figure S18.** Nonlinear curve fitting of CO<sub>2</sub> adsorption isotherms for InOF-1 at 283 K and 295 K.

| <b>GaOF-1</b> |            | <b>Value</b>       | <b>Standard Error</b> |
|---------------|------------|--------------------|-----------------------|
| <b>ln(P)</b>  | <b>a0*</b> | <b>-2202.0793</b>  | <b>16.14383</b>       |
|               | <b>a1*</b> | <b>-77.37474</b>   | <b>0.59823</b>        |
|               | <b>a2*</b> | <b>0.46194</b>     | <b>0.00542</b>        |
|               | <b>a3*</b> | <b>5.45965E-4</b>  | <b>6.51968E-5</b>     |
|               | <b>a4*</b> | <b>-4.47126E-6</b> | <b>4.96664E-7</b>     |
|               | <b>a5*</b> | <b>1.46491E-8</b>  | <b>1.36517E-9</b>     |
|               | <b>b0*</b> | <b>8.98839</b>     | <b>0.0558</b>         |
|               | <b>b1*</b> | <b>0.26947</b>     | <b>0.00209</b>        |
|               | <b>b2*</b> | <b>-0.00168</b>    | <b>1.66948E-5</b>     |
|               | <b>k</b>   | <b>283</b>         | <b>0</b>              |
|               | <b>k</b>   | <b>295</b>         | <b>0</b>              |

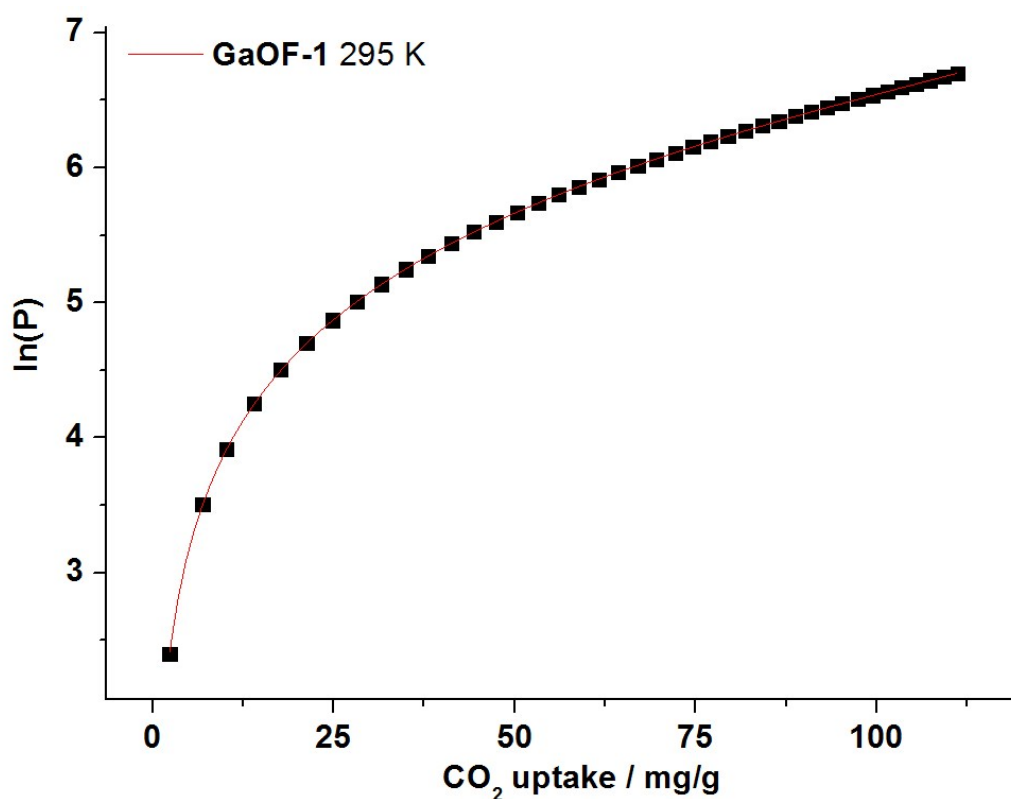
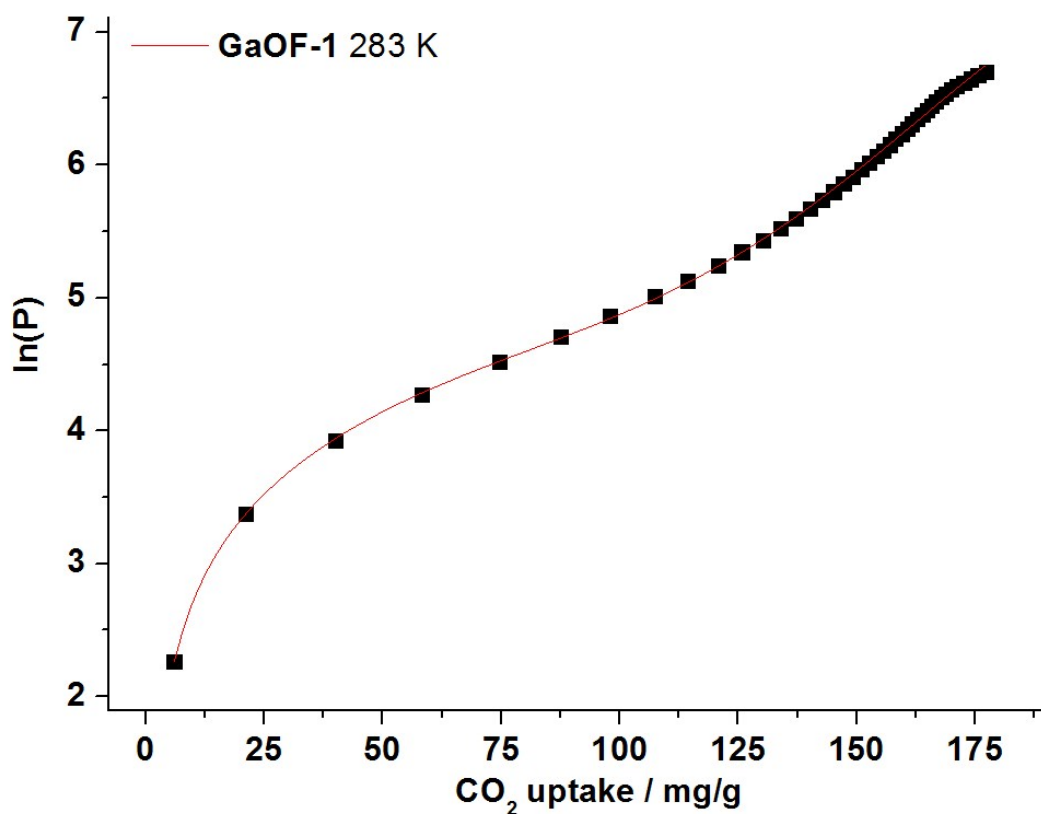


**Figure S19.** Nonlinear curve fitting of CO<sub>2</sub> adsorption isotherms for GaOF-1 at 283 K and 295 K.

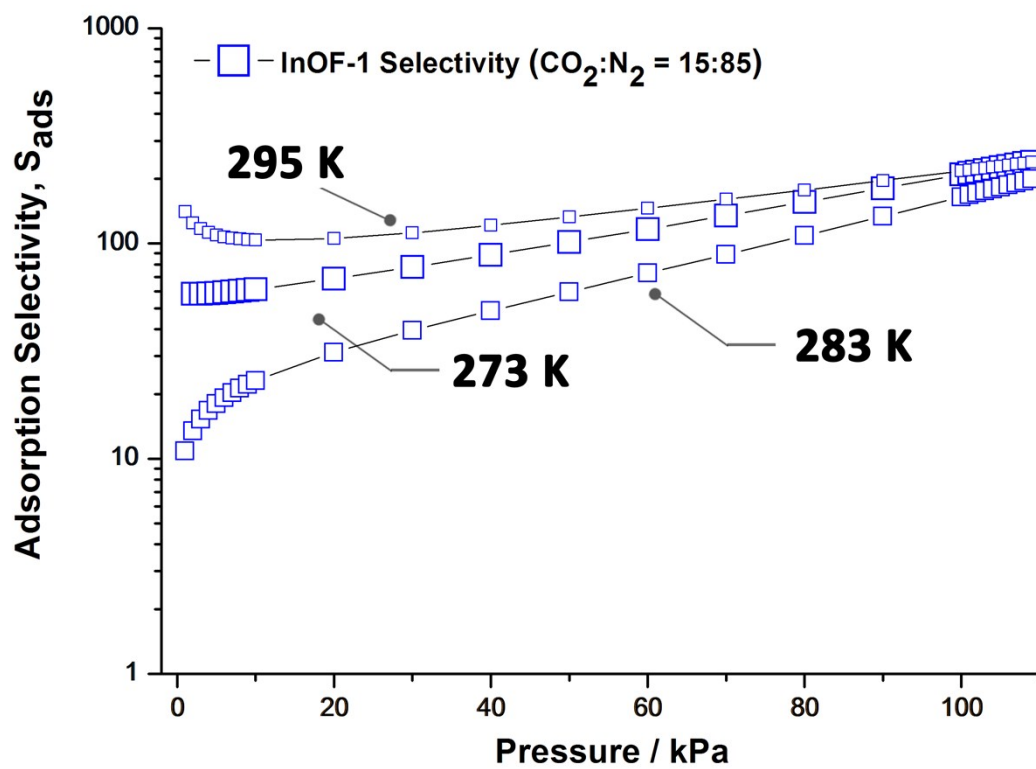


**Figure S20.** The selectivity between  $CO_2$  and  $N_2$  at three different temperatures for InOF-1 with 15:85 mixture.

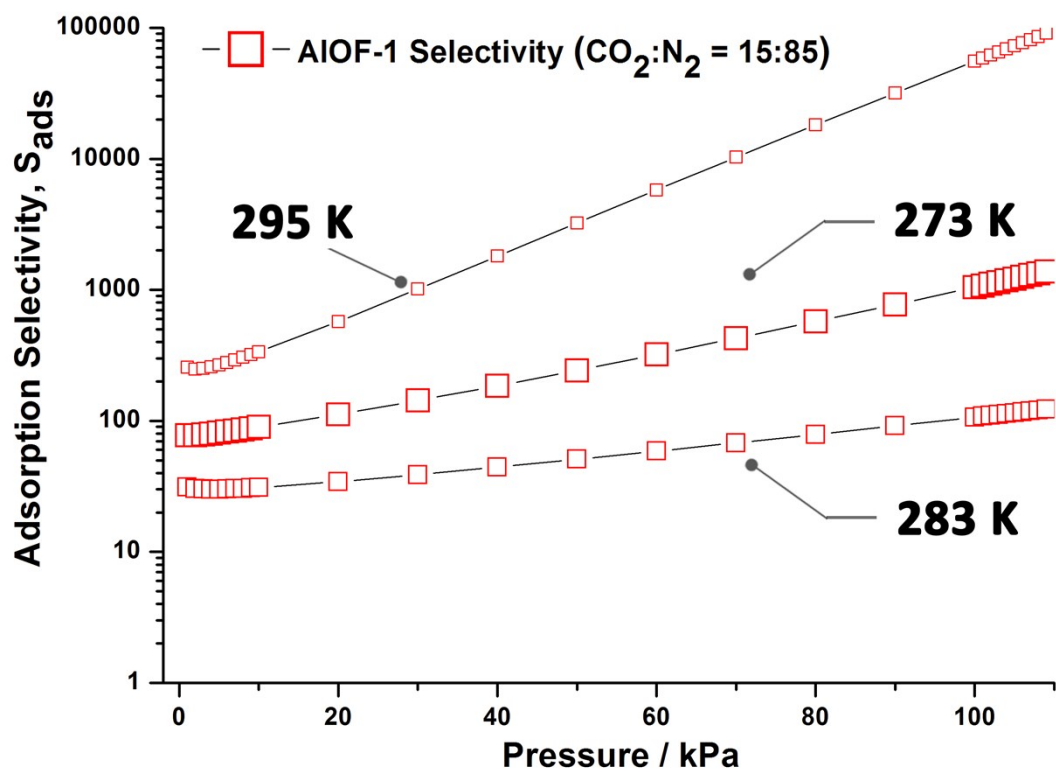


**Figure S21.** The selectivity between CO<sub>2</sub> and N<sub>2</sub> at three different temperatures for AIOF-1 with 15:85 mixture.

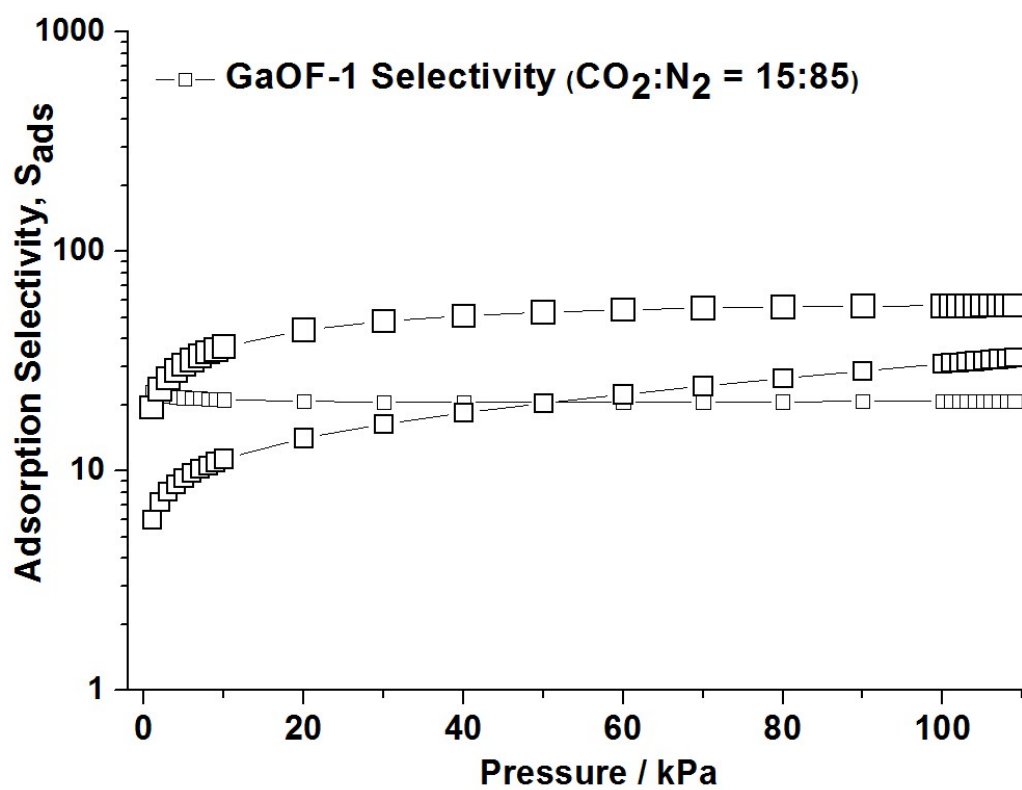


**Figure S22.** The selectivity between CO<sub>2</sub> and N<sub>2</sub> at three different temperatures for GaOF-1 with 15:85 mixture.

## S7. Energy Band Dispersion

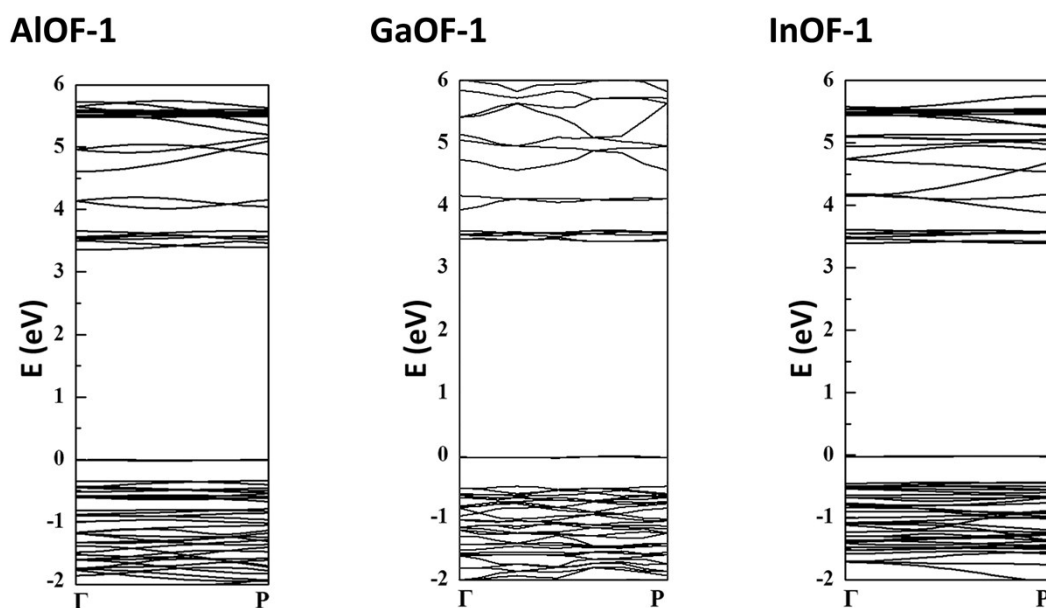


**Figure S23.** Energy band dispersion of AlOF-1, GaOF-1 and InOF-1 along the pore channel direction. The similar energy band gap between these 3 isostructures indicates the similar combining tendency between the host and the CO<sub>2</sub> molecules, consistent well with other theoretically calculated energy-related factors, including the Binding Energy, Zero Point Energy, Thermal Energy and Binding Enthalpy.